Analysis of Dielectric Photonic-Crystal Problems With MLFMA and Schur-Complement Preconditioners

Özgür Ergül, *Member, IEEE*, Tahir Malas, *Member, IEEE*, and Levent Gürel, *Fellow, IEEE*

***Abstract*—We present rigorous solutions of electromagnetics problems involving 3-D dielectric photonic crystals (PhCs). Problems are formulated with recently developed surface integral equations and solved iteratively using the multilevel fast multipole algorithm (MLFMA). For efficient solutions, iterations are accelerated via robust Schur-complement preconditioners. We show that complicated PhC structures can be analyzed with unprecedented efficiency and accuracy by an effective solver based on the combined tangential formulation, MLFMA, and Schur-complement preconditioners.**

***Index Terms*—Multilevel fast multipole algorithm (MLFMA), photonic crystals (PhCs), Schur-complement preconditioners, surface integral equations (SIEs).**

I. Introduction

PHOTONIC CRYSTALS (PhCs) are artificial structures that are usually constructed by periodically arranging dielectric unit cells [1]. They exhibit frequency-selective electromagnetic responses, i.e., their electromagnetic transmission properties change rapidly as a function of frequency. For example, Fig. 1(a) depicts a PhC structure involving periodic dielectric slabs. Depending on the frequency, this relatively simple structure can be transparent and behave like a waveguide, or it can be opaque and inhibit the transmission of electromagnetic waves [2]. Due to its frequency-selective property, this structure can be used as a filter in microwave circuits and antenna systems. Another example, namely, a perforated waveguide (PW), is depicted in Fig. 1(b). This structure is also frequency selective, and it can be used to change the direction of electromagnetic waves in a range of frequencies [3]–[7].

Numerical solutions of transmission problems involving PhC structures are essential to test and improve existing designs prior to their actual realizations. For example, analysis and investigation of PhCs using the finite-element method and the finite-difference time-domain method are quite common in the literature [8]–[11]. Multiple scattering methods are also shown to be particularly useful to analyze perforated waveguides (PWs) [6], [7]. On the other hand, surface integral equations (SIEs) based on the equivalence principle are rarely applied to PhCs [12]–[14]. In particular, investigation of 3-D structures with finite dimensions via SIEs is not common in the literature. In fact, traditional surface formulations, such as the Poggio-Miller–Chang–Harrington–Wu–Tsai (PMCHWT) formulation [15]–[17] and the Müller formulation [18], may not be very suitable for solving transmission problems involving complicated PhC structures. PhCs are usually large in terms of wavelength, and their surface discretizations lead to relatively large matrix equations that cannot be directly solved. Hence, iterative solvers are required for surface formulations of PhC problems. However, the PMCHWT formulation usually leads to ill-conditioned matrix equations, and thus, to very slow convergence rates for iterative solutions of PhC problems. In addition, the resonating nature of PhC structures further inhibits the rapid convergence of iterations. The Müller formulation may lead to well-conditioned matrix equations, but the accuracy of this formulation is usually very poor, especially for PhCs with sharp edges and corners, or those having small details with respect to wavelength. As a result, it is not surprising that SIEs have not been very popular for analyzing PhCs.

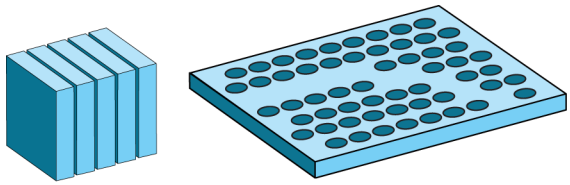

Fig. 1. Examples of PhC problems: (a) periodic slabs and (b) perforated waveguide.

In this paper, we present fast and accurate solutions of PhC problems using a rigorous solver based on the combination of novel surface formulations, the multilevel fast multiple algorithm (MLFMA) [19], and robust preconditioning techniques. Problems are formulated with the combined tangential formulation (CTF) [20], the combined normal formulation (CNF) [20], the modified normal Müller formulation (MNMF) [21], and the electric and magnetic current combined-field integral equation (JMCFIE) [22], all of which have been recently

Manuscript received July 22, 2010; revised October 29, 2010; accepted December 16, 2010. Date of publication January 13, 2011; date of current version March 07, 2011.

Ö. Ergül was with the Department of Electrical and Electronics Engineering, Bilkent University, Bilkent 06800, Ankara, Turkey. He is now with the Department of Mathematics and Statistics, University of Strathclyde, Glasgow G1 1XH, UK.

T. Malas was with the Department of Electrical and Electronics Engineering, Bilkent University, Bilkent 06800, Ankara, Turkey. He is now with the Department of Electrical and Computer Engineering, The University of Texas at Austin, Austin, TX 78712 USA.

L. Gürel is with the Computational Electromagnetics Research Center, and Center and the Department of Electrical and Electronics Engineering, Bilkent University, Bilkent 06800, Ankara, Turkey (e-mail: lgurel@bilkent.edu.tr).

Color versions of one or more of the figures in this paper are available online at http://ieeexplore.ieee.org.

Digital Object Identifier 10.1109/JLT.2011.2106196

TABLE I
ELECTROMAGNETIC PROBLEMS INVOLVING PSS

Problem	Dimensions of Slabs	Number of Slabs	Unknowns
PS1	0.41×2×2 cm	5	38,700
PS2	0.41×2×2 cm	10	77,400
PS3	0.41×4×4 cm	5	131,460
PS4	0.41×4×4 cm	10	262,920

TABLE II
ELECTROMAGNETIC PROBLEMS INVOLVING PWS

Problem	Size of Structure	Number of Holes	Unknowns
PW1	0.6×5×10 cm	38	27,798
PW2	0.6×15×20 cm	272	162,420
PW3	0.6×26×34 cm	828	475,782
PW4	0.6×29×38 cm	1042	597,462

developed for stable formulations of 3-D dielectric objects. SIEs are discretized with the Rao–Wilton–Glisson (RWG) [23] functions, and the resulting dense matrix equations are solved iteratively using MLFMA. Iterative solutions are accelerated by robust Schur-complement preconditioning techniques, namely, approximate and iterative Schur preconditioners (ISPs). Comparisons show that transmission problems involving 3-D PhCs can be analyzed with unprecedented efficiency and accuracy by using an integral-equation solver based on CTF, MLFMA, and Schur-complement preconditioners.

Solution techniques presented in this paper are demonstrated on two different types of PhC structures. Our main aim is to solve complicated PhC problems, such as the PW depicted in Fig. 1(b). Hence, we present our efforts on various PWs with different sizes. At the same time, as a major advantage of this study, the developed solvers are not limited to the shape of the PhCs, hence, they can be applied to arbitrary PhC structures. Therefore, we also present the solution of transmission problems involving periodic dielectric slabs, such as the one depicted in Fig. 1(a), which have relatively simple shapes but involve multiple bodies.

The rest of the paper is organized as follows: In Section II, we briefly present the basic properties of the PhC problems investigated in this paper. Surface formulations and their solutions with MLFMA are summarized in Section III. Section IV is devoted to Schur-complement preconditioners, which are essential for efficient solutions of PhC problems. Numerical results are presented in Section V, followed by our concluding remarks in Section VI. All solutions are performed in the frequency domain involving time-harmonic electromagnetic fields with the $e^{-i\omega t}$ time dependence.

II. PHC STRUCTURES

Table I lists the details of the periodic-slabs (PSs) problems, involving periodically arranged rectangular slabs with a relative permittivity of 4.8 located in free space. The slabs have dimensions of either 0.41 cm × 2 cm × 2 cm or 0.41 cm × 4 cm × 4 cm, and there are either 5 or 10 slabs, depending on the problem. The distance between the slabs is fixed at 0.09 cm. With the given dimensions, PSs resonate at around 30 GHz and become opaque to electromagnetic waves. The resonance also causes the ill-conditioning of the resulting matrix equations. Hence, we analyze the iteration counts and solution times, particularly at 30 GHz. PSs are illuminated by a Hertzian dipole. Discretizations with the RWG functions on $\lambda_O/10$ triangles, where λ_O is the wavelength in free space, lead to matrix equations involving 38 700–262 920 unknowns.

Table II lists the details of the PW problems. Each problem involves a dielectric slab with a relative permittivity of 12.0 in free space. The holes are arranged on each slab such that electromagnetic waves can be transmitted from one of the short edges to a neighboring long edge. As depicted in Fig. 1(b), some of the holes in the regular grids are missing to allow the propagation of waves inside the structures. The size of the slabs varies from 5 cm × 10 cm to 29 cm × 38 cm with a constant thickness of 0.6 cm. The total number of holes changes accordingly, from 38 to 1042. The distance between the centers of the holes is 1 cm, whereas the radius of each hole is 0.29 cm. With these dimensions, transmission is high between 7 and 9 GHz. Specifically, the smaller problems PW1 and PW2 are solved at 8.25 GHz, whereas PW3 and PW4 are solved at 7.6 GHz, i.e., when the transmission is maximized according to numerical results. Similar to the PSs, PWs are excited with Hertzian dipoles. Discretizations with the RWG functions on $\lambda_O/20$ triangles lead to matrix equations involving 27 798–597 462 unknowns. These fine triangulations are required for accurate modeling of the circular holes.

III. INTEGRAL EQUATIONS AND SOLUTIONS

In this section, we summarize recently developed integral-equation formulations and their solutions with MLFMA.

A. Formulation

SIEs are based on the equivalence principle, where equivalent currents $\boldsymbol{J}(\boldsymbol{r}) = \hat{\boldsymbol{n}} \times \boldsymbol{H}(\boldsymbol{r})$ and $\boldsymbol{M}(\boldsymbol{r}) = -\hat{\boldsymbol{n}} \times \boldsymbol{E}(\boldsymbol{r})$ are defined on the surface of the object. Using the boundary conditions, equivalent currents, hence the electromagnetic fields inside and outside the object, can be calculated. Depending on the tested field (electric or magnetic), the location (from inside or outside), and the method (direct or rotational) of testing the boundary conditions, eight different integral equations can be obtained [24]. Combining these integral equations, one can derive various dielectric formulations, such as PMCHWT [15]–[17], Müller [18], CTF, CNF, MNMF, and JMCFIE [20]–[22], to solve electromagnetics problems. Efficiency and accuracy of the solutions naturally depend on the formulation in addition to various properties of the problem, e.g., the shape and dielectric constants of the object as well as the excitation. For example, in earlier studies, we showed that JMCFIE is superior to other formulations for relatively simple objects, such as the PhC structure in Fig. 1, when simple preconditioners are used [24]. The same formulation is also very successful in terms of accuracy and efficiency for smooth and large objects. On the other hand, as demonstrated in this paper, JMCFIE may not be the most appropriate formulation for more difficult problems, such as a PW, that require robust preconditioners.

Surface formulations and their solutions are extensively discussed in [20] and [24]. In this paper, we will consider only their

discretized forms. Each formulation involves a distinct combination of discrete versions of three surface operators, i.e.,

$$\mathcal{T}_u\{\boldsymbol{X}\}(\boldsymbol{r}) = ik_u \int_S d\boldsymbol{r}' \boldsymbol{X}(\boldsymbol{r}') g_u(\boldsymbol{r},\boldsymbol{r}') + \frac{i}{k_u}\int_S d\boldsymbol{r}' \nabla' \cdot \boldsymbol{X}(\boldsymbol{r}') \nabla g_u(\boldsymbol{r},\boldsymbol{r}') \quad (1)$$

$$\mathcal{K}_{\mathrm{PV},u}\{\boldsymbol{X}\}(\boldsymbol{r}) = \int_{\mathrm{PV},S} d\boldsymbol{r}' \boldsymbol{X}(\boldsymbol{r}') \times \nabla' g_u(\boldsymbol{r},\boldsymbol{r}') \quad (2)$$

$$\mathcal{I}\{\boldsymbol{X}\}(\boldsymbol{r}) = \boldsymbol{X}(\boldsymbol{r}) \quad (3)$$

where $\boldsymbol{X}$ is either the equivalent electric current $\boldsymbol{J}$ or the equivalent magnetic current $\boldsymbol{M}$. In (1) and (2), PV indicates the principal value of the integral, $k_u = \omega\sqrt{\mu_u \epsilon_u}$ is the wavenumber, and

$$g_u(\boldsymbol{r},\boldsymbol{r}') = \frac{\exp(ik_u R)}{4\pi R}, \qquad (R = |\boldsymbol{r} - \boldsymbol{r}'|) \quad (4)$$

denotes the homogeneous-space Green's function associated with the outside ($u = O$) or inside ($u = I$) of the object.

B. Discretization

Discretizations of surface formulations for homogeneous dielectric objects using a set of basis functions $\boldsymbol{b}_n$ ($n = 1, 2, \ldots, N$) and a set of testing functions $\boldsymbol{t}_m$ ($m = 1, 2, \ldots, N$) lead to $2N \times 2N$ dense matrix equations in the form of

$$\begin{bmatrix} \bar{\boldsymbol{Z}}_{11} & \bar{\boldsymbol{Z}}_{12} \\ \bar{\boldsymbol{Z}}_{21} & \bar{\boldsymbol{Z}}_{22} \end{bmatrix} \cdot \begin{bmatrix} \boldsymbol{a}_J \\ \boldsymbol{a}_M \end{bmatrix} = \begin{bmatrix} \boldsymbol{v}_1 \\ \boldsymbol{v}_2 \end{bmatrix} \quad (5)$$

where $\bar{\boldsymbol{Z}}_{11}$, $\bar{\boldsymbol{Z}}_{12}$, $\bar{\boldsymbol{Z}}_{21}$, $\bar{\boldsymbol{Z}}_{22} \in \mathbb{C}^{N\times N}$. Solutions of (5) via Krylov-subspace algorithms provide expansion coefficients $\boldsymbol{a}_J$ and $\boldsymbol{a}_M$ for equivalent electric and magnetic currents, respectively. Then, using the coefficients, scattered electric and magnetic fields can be calculated everywhere.

There are infinitely many surface formulations for electromagnetics problems involving dielectric objects. Some of these formulations are known to be stable and provide accurate results, although the efficiency and accuracy of the solution may vary significantly, depending on the formulation and the discretization. In this paper, we first consider four recently developed formulations, namely, CTF, CNF, MNMF, and JMCFIE. Considering the initial experiments, CTF and JMCFIE are also employed to solve PhC problems.

CTF is a tangential formulation [20], where boundary conditions are tested directly by sampling the tangential components of the electric and magnetic fields on the surface. Matrix elements are derived as follows:

$$\bar{\boldsymbol{Z}}_{11}^{\mathrm{CTF}} = \bar{\boldsymbol{Z}}_{22}^{\mathrm{CTF}} = \bar{\boldsymbol{T}}_O^T + \bar{\boldsymbol{T}}_I^T \quad (6)$$

$$\bar{\boldsymbol{Z}}_{12}^{\mathrm{CTF}} = -\eta_O^{-1}\bar{\boldsymbol{K}}_{\mathrm{PV},O}^T - \eta_I^{-1}\bar{\boldsymbol{K}}_{\mathrm{PV},I}^T - \frac{1}{2}\left(\eta_O^{-1} - \eta_I^{-1}\right)\bar{\boldsymbol{I}}^N \quad (7)$$

$$\bar{\boldsymbol{Z}}_{21}^{\mathrm{CTF}} = \eta_O\bar{\boldsymbol{K}}_{\mathrm{PV},O}^T + \eta_I\bar{\boldsymbol{K}}_{\mathrm{PV},I}^T + \frac{1}{2}(\eta_O - \eta_I)\bar{\boldsymbol{I}}^N \quad (8)$$

where

$$\bar{\boldsymbol{T}}_u^T[m,n] = \langle \boldsymbol{t}_m(\boldsymbol{r}), \mathcal{T}_u\{\boldsymbol{b}_n\}(\boldsymbol{r})\rangle \quad (9)$$

$$\bar{\boldsymbol{K}}_{\mathrm{PV},u}^T[m,n] = \langle \boldsymbol{t}_m(\boldsymbol{r}), \mathcal{K}_{\mathrm{PV},u}\{\boldsymbol{b}_n\}(\boldsymbol{r})\rangle \quad (10)$$

$$\bar{\boldsymbol{I}}^N[m,n] = \langle \boldsymbol{t}_m(\boldsymbol{r}), \hat{\boldsymbol{n}} \times \boldsymbol{b}_n(\boldsymbol{r})\rangle \quad (11)$$

and $\eta_u = \sqrt{\mu_u/\epsilon_u}$ for $u = O$ and $u = I$. In terms of the stability and the conditioning of the resulting matrix equations, CTF is an improved version of the well-known PMCHWT formulation.

CNF is a normal formulation [20], where fields are tested after they are projected onto the surface by using the outward normal vector. Matrix elements can be written as follows:

$$\bar{\boldsymbol{Z}}_{11}^{\mathrm{CNF}} = \bar{\boldsymbol{Z}}_{22}^{\mathrm{CNF}} = \bar{\boldsymbol{K}}_{\mathrm{PV},O}^N - \bar{\boldsymbol{K}}_{\mathrm{PV},I}^N - \bar{\boldsymbol{I}}^T \quad (12)$$

$$\bar{\boldsymbol{Z}}_{12}^{\mathrm{CNF}} = \eta_O^{-1}\bar{\boldsymbol{T}}_O^N - \eta_I^{-1}\bar{\boldsymbol{T}}_I^N \quad (13)$$

$$\bar{\boldsymbol{Z}}_{21}^{\mathrm{CNF}} = -\eta_O\bar{\boldsymbol{T}}_O^N + \eta_I\bar{\boldsymbol{T}}_I^N \quad (14)$$

where

$$\bar{\boldsymbol{T}}^N[m,n] = \langle \boldsymbol{t}_m(\boldsymbol{r}), \hat{\boldsymbol{n}} \times \mathcal{T}\{\boldsymbol{b}_n\}(\boldsymbol{r})\rangle \quad (15)$$

$$\bar{\boldsymbol{K}}_{\mathrm{PV},u}^N[m,n] = \langle \boldsymbol{t}_m(\boldsymbol{r}), \hat{\boldsymbol{n}} \times \mathcal{K}_{\mathrm{PV},u}\{\boldsymbol{b}_n\}(\boldsymbol{r})\rangle \quad (16)$$

$$\bar{\boldsymbol{I}}^T[m,n] = \langle \boldsymbol{t}_m(\boldsymbol{r}), \boldsymbol{b}_n(\boldsymbol{r})\rangle. \quad (17)$$

MNMF is another normal formulation [21] obtained by changing the scaling of the integral equations in CNF such that

$$\bar{\boldsymbol{Z}}_{11}^{\mathrm{MNMF}} = \frac{1}{(\mu_O + \mu_I)}\left(\mu_O\bar{\boldsymbol{K}}_{\mathrm{PV},O}^N - \mu_I\bar{\boldsymbol{K}}_{\mathrm{PV},I}^N\right) - \frac{1}{2}\bar{\boldsymbol{I}}^T \quad (18)$$

$$\bar{\boldsymbol{Z}}_{12}^{\mathrm{MNMF}} = \frac{1}{(\mu_O + \mu_I)}\left(\mu_O\eta_O^{-1}\bar{\boldsymbol{T}}_O^N - \mu_I\eta_I^{-1}\bar{\boldsymbol{T}}_I^N\right) \quad (19)$$

$$\bar{\boldsymbol{Z}}_{21}^{\mathrm{MNMF}} = -\frac{1}{(\epsilon_O + \epsilon_I)}\left(\epsilon_O\eta_O\bar{\boldsymbol{T}}_O^N - \epsilon_I\eta_I\bar{\boldsymbol{T}}_I^N\right) \quad (20)$$

$$\bar{\boldsymbol{Z}}_{22}^{\mathrm{MNMF}} = \frac{1}{(\epsilon_O + \epsilon_I)}\left(\epsilon_O\bar{\boldsymbol{K}}_{\mathrm{PV},O}^N - \epsilon_I\bar{\boldsymbol{K}}_{\mathrm{PV},I}^N\right) - \frac{1}{2}\bar{\boldsymbol{I}}^T. \quad (21)$$

We note that the matrix equations obtained with MNMF involve nonidentical diagonal blocks, as opposed to those obtained with CTF and CNF. Both CNF and MNMF are improved versions of the well-known Müller formulation.

Finally, JMCFIE is a mixed formulation [22], which can be obtained by combining CTF and CNF, i.e.,

$$\bar{\boldsymbol{Z}}_{11}^{\mathrm{JMCFIE}} = \bar{\boldsymbol{Z}}_{22}^{\mathrm{JMCFIE}} = \bar{\boldsymbol{Z}}_{11}^{\mathrm{CTF}} + \bar{\boldsymbol{Z}}_{11}^{\mathrm{CNF}} \quad (22)$$

$$\bar{\boldsymbol{Z}}_{12}^{\mathrm{JMCFIE}} = \bar{\boldsymbol{Z}}_{12}^{\mathrm{CTF}} + \bar{\boldsymbol{Z}}_{12}^{\mathrm{CNF}} \quad (23)$$

$$\bar{\boldsymbol{Z}}_{21}^{\mathrm{JMCFIE}} = \bar{\boldsymbol{Z}}_{21}^{\mathrm{CTF}} + \bar{\boldsymbol{Z}}_{21}^{\mathrm{CNF}}. \quad (24)$$

Applying a Galerkin scheme and using the same set of RWG functions as the basis and testing functions, CTF involves weakly tested identity operators. Hence, CTF is practically a first-kind integral-equation formulation, and it produces ill-conditioned matrix equations without preconditioning. Nevertheless, CTF is usually more accurate than the normal and mixed formulations. CNF, MNMF, and JMCFIE involve well-tested identity operators and produce better conditioned matrix equations than CTF. Unfortunately, due to the excessive discretization error of the identity operator [25], the accuracy

of CNF, MNMF, and JMCFIE can be poor, especially when the contrast of the object is high and/or the object involves sharp edges and corners.

C. Solutions With MLFMA

Dense matrix equations obtained from integral-equation formulations can be solved efficiently with MLFMA [19]. Using this algorithm, matrix–vector multiplications, i.e., interactions between basis and testing functions, are performed in a group-by-group manner. A multilevel tree structure is obtained by placing the object in a cubic box and recursively dividing the computational domain into subboxes. Then, only $\mathcal{O}(N)$ near-field interactions are calculated directly and stored in memory, whereas the rest of the interactions (far-field interactions) are calculated in three stages, called aggregation, translation, and disaggregation. During the aggregation stage, the radiation patterns of boxes are calculated from the bottom to the top of the tree structure. Then, the incoming fields for all boxes are obtained through translation and disaggregation stages. Due to the oscillatory nature of the Helmholtz equation, the sampling rate for the radiation and receiving patterns depends on the size of the boxes, with respect to the wavelength associated with the medium. Hence, local Lagrange interpolation and anterpolation methods are employed to match the different sampling rates of the consecutive levels. In addition, two versions of MLFMA, i.e., with different sampling rates, are required to perform the matrix–vector multiplications related to the inner and outer media. The application of MLFMA to surface formulations of dielectric objects is detailed in [24] and [27].

IV. Schur-Complement Preconditioning

Approximating the dense matrix in (5) by a sparse near-field matrix involving only the near-field interactions, preconditioning techniques developed for sparse systems can be adapted to solve integral-equation formulations. However, standard algebraic preconditioners, such as the methods based on incomplete LU (ILU) factorizations, often fail for indefinite partitioned systems that are not diagonally dominant [26], [28]. A similar behavior is observed for linear systems obtained from surface formulations [29]. Nevertheless, it is possible to obtain robust preconditioners using the Schur-complement reduction. This method decomposes the solution of the 2×2 partitioned near-field system

$$\begin{bmatrix} \bar{\boldsymbol{Z}}_{\mathrm{NF},11} & \bar{\boldsymbol{Z}}_{\mathrm{NF},12} \\ \bar{\boldsymbol{Z}}_{\mathrm{NF},21} & \bar{\boldsymbol{Z}}_{\mathrm{NF},22} \end{bmatrix} \cdot \begin{bmatrix} \boldsymbol{x} \\ \boldsymbol{y} \end{bmatrix} = \begin{bmatrix} \boldsymbol{f} \\ \boldsymbol{g} \end{bmatrix} \tag{25}$$

into solutions of two subsystems. First, $\boldsymbol{y}$ is found by solving

$$\bar{\boldsymbol{S}} \cdot \boldsymbol{y} = \boldsymbol{g} - \bar{\boldsymbol{Z}}_{\mathrm{NF},21} \cdot (\bar{\boldsymbol{Z}}_{\mathrm{NF},11})^{-1} \cdot \boldsymbol{f} \tag{26}$$

where

$$\bar{\boldsymbol{S}} = \bar{\boldsymbol{Z}}_{\mathrm{NF},22} - \bar{\boldsymbol{Z}}_{\mathrm{NF},21} \cdot (\bar{\boldsymbol{Z}}_{\mathrm{NF},11})^{-1} \cdot \bar{\boldsymbol{Z}}_{\mathrm{NF},12} \tag{27}$$

is the Schur complement. Then, $\boldsymbol{x}$ can be found by solving

$$\bar{\boldsymbol{Z}}_{\mathrm{NF},11} \cdot \boldsymbol{x} = \boldsymbol{f} - \bar{\boldsymbol{Z}}_{\mathrm{NF},12} \cdot \boldsymbol{y}. \tag{28}$$

In a variety of applications that yield partitioned systems, preconditioners developed with some approximations to (26) and (28) have been shown to demonstrate successful results [26].

The reduced systems (26) and (28) can be solved in two different ways, leading to two preconditioning approaches. In the first approach, systems are solved directly, but the inverses of $\bar{\boldsymbol{Z}}_{\mathrm{NF},11}$ and $\bar{\boldsymbol{S}}$ are approximated during solutions. The resulting preconditioner is called the approximate Schur preconditioner (ASP). We note that the approximate inverse of $\bar{\boldsymbol{Z}}_{\mathrm{NF},11}$ is used also on the right-hand sides of (26) and (27), in addition to the solution of (28). In the second approach, (26) and (28) are solved iteratively, and the resulting preconditioner is called the ISP. For ISP, we refer to iterative solutions related to the two reduced systems as "inner solutions" and the solution related to the actual system (5) as the "outer solution." If the numbers of inner iterations for the reduced systems are not fixed at a constant, a flexible solver, such as the flexible generalized minimal residual (FGMRES) method, should be used for the outer solution [26]. Since the near-field system usually inherits the inconvenient features of the dense system, it is vital to use inner preconditioners to accelerate the solutions of the reduced systems for robustness.

ASP and ISP have some pros and cons in terms of preconditioning cost and efficiency. Because of the inner solutions, ISP has a higher application cost than ASP. However, in the case of ASP, high-quality approximate inverses should be constructed for both $\bar{\boldsymbol{Z}}_{\mathrm{NF},11}$ and the Schur complement $\bar{\boldsymbol{S}}$. This can be tough, particularly for the Schur complement $\bar{\boldsymbol{S}}$. As an important advantage of ISP, when the approximate inverses are used as preconditioners to the inner solutions of ISP, the high-quality requirement can be relaxed. Additionally, with inner iterative solutions, it is easier to balance the solution accuracy of the two reduced systems and, thus, eliminate redundant computation [30].

Since the success of ASP and ISP will depend on the quality of the approximate inverses (which can be used as inner preconditioners for ISP), we need to analyze possible approaches to approximate the inverses of $\bar{\boldsymbol{Z}}_{\mathrm{NF},11}$ and $\bar{\boldsymbol{S}}$.

A. Approximate Inverse of $\bar{\boldsymbol{Z}}_{\mathrm{NF},11}$

For efficiency and to limit the memory requirement, the approximate inverses should be sparse. For $\bar{\boldsymbol{Z}}_{\mathrm{NF},11}$, a sparse approximate inverse $\mathrm{SAI}\{\bar{\boldsymbol{Z}}_{11}\}$ can be constructed by retaining the nonzero pattern of the partition. To demonstrate the effectiveness of $\mathrm{SAI}\{\bar{\boldsymbol{Z}}_{11}\}$, we iteratively solve (28) for the PhC problems PS4 and PW2 listed in Tables I and II, respectively. In Figs. 2 and 3, we compare the generalized minimal residual (GMRES) solutions without preconditioning (no preconditioner: NP) and with $\mathrm{SAI}\{\bar{\boldsymbol{Z}}_{11}\}$. We analyze convergence for the first ten iterations since a rough solution, generally up to 0.1 residual error, is shown to be sufficient to yield a successful preconditioner for ISP [26]. We observe that $\mathrm{SAI}\{\bar{\boldsymbol{Z}}_{11}\}$ significantly accelerates the solutions, except for the only case when MNMF is applied to the PW. In this case, the preconditioner slightly increases the number of iterations. Nevertheless, it becomes possible to obtain 0.1 residual error quite rapidly (e.g., in fewer than ten iterations) in all cases when $\mathrm{SAI}\{\bar{\boldsymbol{Z}}_{11}\}$ is employed, proving the effectiveness of this preconditioner for the reduced system (28).

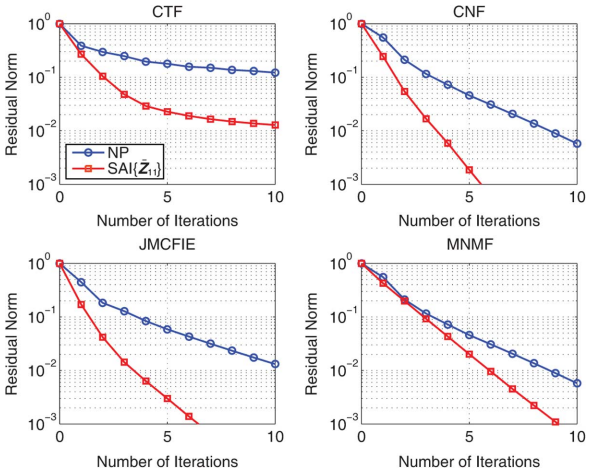

Fig. 2. Iterative solutions of (28) without preconditioning and with $\mathrm{SAI}\{\bar{\boldsymbol{Z}}_{11}\}$ for the problem PS4 involving 262 920 unknowns.

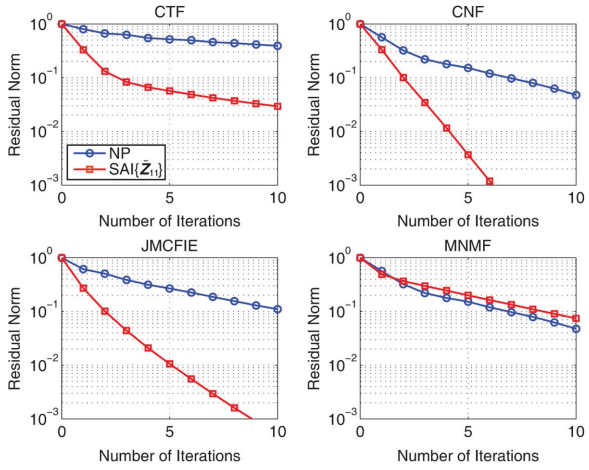

Fig. 3. Iterative solutions of (28) without preconditioning and with $\mathrm{SAI}\{\bar{\boldsymbol{Z}}_{11}\}$ for the problem PW2 involving 162 420 unknowns.

Finally, we note that, in the case of ASP, $\mathrm{SAI}\{\bar{\boldsymbol{Z}}_{11}\}$ is used to approximate $\bar{\boldsymbol{Z}}_{11}$ in the direct solution of (28). In the case of ISP, however, $\mathrm{SAI}\{\bar{\boldsymbol{Z}}_{11}\}$ is used as an inner preconditioner for the iterative solution of (28). For both ASP and ISP, the reduced system (26) can be modified as follows:

$$\bar{\boldsymbol{S}} \cdot \boldsymbol{y} = \boldsymbol{g} - \bar{\boldsymbol{Z}}_{\mathrm{NF},21} \cdot \mathrm{SAI}\{\bar{\boldsymbol{Z}}_{11}\} \cdot \boldsymbol{f} \tag{29}$$

where

$$\bar{\boldsymbol{S}} = \bar{\boldsymbol{Z}}_{\mathrm{NF},22} - \bar{\boldsymbol{Z}}_{\mathrm{NF},21} \cdot \mathrm{SAI}\{\bar{\boldsymbol{Z}}_{11}\} \cdot \bar{\boldsymbol{Z}}_{\mathrm{NF},12}. \tag{30}$$

In other words, we approximate the inverse of $\bar{\boldsymbol{Z}}_{\mathrm{NF},11}$ on the right-hand sides of (26) and (27).

B. Approximate Inverses of the Schur Complement $\bar{\boldsymbol{S}}$

We investigate three different approaches to approximate the inverse of the Schur complement $\bar{\boldsymbol{S}}$. First, it is possible to approximate $\bar{\boldsymbol{S}}$ with block-diagonal partitions, which consist of the self-interactions of the lowest level clusters in MLFMA. The inverse of $\bar{\boldsymbol{S}}$ can be approximated as follows:

$$\mathrm{BDI}\{\bar{\boldsymbol{S}}\} = (\bar{\boldsymbol{B}}_{22} - \bar{\boldsymbol{B}}_{21} \cdot (\bar{\boldsymbol{B}}_{11})^{-1} \cdot \bar{\boldsymbol{B}}_{12})^{-1} \tag{31}$$

where B_{ij} represents the block-diagonal part of Z_{ij} for $i = 1, 2$ and $j = 1, 2$. In (31), inverse operations can be performed directly without the need for an approximation, and the resulting matrix $\mathrm{BDI}\{\bar{\boldsymbol{S}}\}$ is also block diagonal.

A second approach is to omit the second term in the right-hand side of (30), and to approximate the inverse of $\bar{\boldsymbol{S}}$ with the sparse approximate inverse of $\bar{\boldsymbol{Z}}_{\mathrm{NF},22}$, i.e., $\mathrm{SAI}\{\bar{\boldsymbol{Z}}_{22}\}$. Since $\bar{\boldsymbol{Z}}_{\mathrm{NF},22} = \bar{\boldsymbol{Z}}_{\mathrm{NF},11}$ for all formulations except MNMF, $\mathrm{SAI}\{\bar{\boldsymbol{Z}}_{11}\}$ can be used to approximate the inverse of $\bar{\boldsymbol{S}}$. This approach has the advantage of devising a preconditioner for the dense system (5) by constructing only one sparse approximate inverse. Despite this important advantage, $\mathrm{SAI}\{\bar{\boldsymbol{Z}}_{11}\}$ fails to provide an accurate approximation to the inverse of $\bar{\boldsymbol{S}}$, particularly for high-contrast dielectric objects. Hence, a better approach is to approximate $\bar{\boldsymbol{S}}$ via approximate matrix–matrix multiplications as follows:

$$\tilde{\boldsymbol{S}} = \bar{\boldsymbol{Z}}_{\mathrm{NF},22} - \bar{\boldsymbol{Z}}_{\mathrm{NF},21} \odot \mathrm{SAI}\{\bar{\boldsymbol{Z}}_{11}\} \odot \bar{\boldsymbol{Z}}_{\mathrm{NF},12} \tag{32}$$

where $\odot$ represents the approximate matrix–matrix multiplications. Then, the sparse approximate inverse of $\tilde{\boldsymbol{S}}$, i.e., $\mathrm{SAI}\{\tilde{\boldsymbol{S}}\}$, can be calculated efficiently by preserving the near-field pattern.

In the case of ASP, the aforementioned approximate inverses, i.e., $\mathrm{BDI}\{\bar{\boldsymbol{S}}\}$, $\mathrm{SAI}\{\bar{\boldsymbol{Z}}_{22}\}$, and $\mathrm{SAI}\{\tilde{\boldsymbol{S}}\}$, can be used directly to approximate the inverse of $\bar{\boldsymbol{S}}$ in (29). In the case of ISP, however, they are used as preconditioners for the iterative solution of (29). We note that $\bar{\boldsymbol{S}}$ is not generated explicitly using (30) even when (29) is solved iteratively. Instead, sparse matrix–vector multiplications with $\bar{\boldsymbol{Z}}_{\mathrm{NF},21}$, $\mathrm{SAI}\{\bar{\boldsymbol{Z}}_{11}\}$, and $\bar{\boldsymbol{Z}}_{\mathrm{NF},12}$, are performed efficiently.

In order to compare the different approaches to approximate the inverse of $\bar{\boldsymbol{S}}$, Figs. 4 and 5 present the solution of (29) with GMRES for the PhC problems PS4 and PW2 listed in Tables I and II, respectively. We consider the NP case in addition to three preconditioned solutions when the approximate inverses are employed as preconditioners. First, we observe that the solution of (29) is more difficult than the solution of (28). In particular, it is not possible to attain fast convergence for the normal formulations CNF and MNMF. Among the three approximate inverses, $\mathrm{SAI}\{\tilde{\boldsymbol{S}}\}$ performs the best. This preconditioner significantly accelerates the solutions for the PSs problems formulated with CTF and JMCFIE. On the other hand, for the PW problem involving a high-contrast object, attaining fast convergence is difficult even with $\mathrm{SAI}\{\tilde{\boldsymbol{S}}\}$, and all solutions start to stagnate after the first five iterations. Hence, it is wise to set a low threshold for the maximum number of inner iterations to avoid wasted efforts in ISP.

V. Solutions of PhC Problems

Initial experiments show that CTF and JMCFIE are more appropriate than CNF and MNMF for the solution of PhC problems. As discussed in Section III, CTF is more accurate than the other three formulations. In addition, as demonstrated in Section IV, Schur-complement preconditioners works well for CTF. Hence, CTF is a good candidate for the fast and accurate solution of PhC problems. JMCFIE is another formulation that seems to be accelerated easily with Schur-complement preconditioners. In fact, this formulation provides more accurate

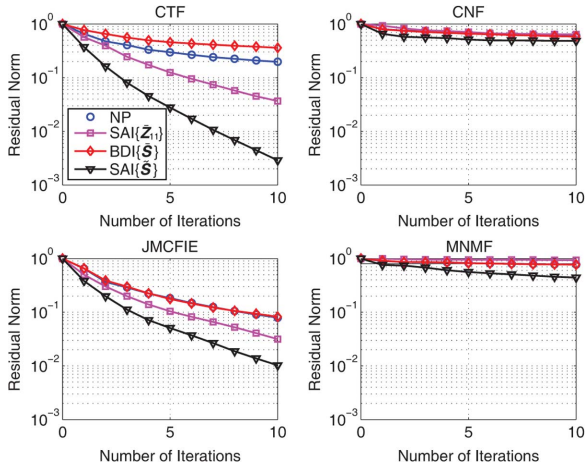

Fig. 4. Iterative solutions of (29) without preconditioning and with various preconditioners for the problem PS4 involving 262 920 unknowns.

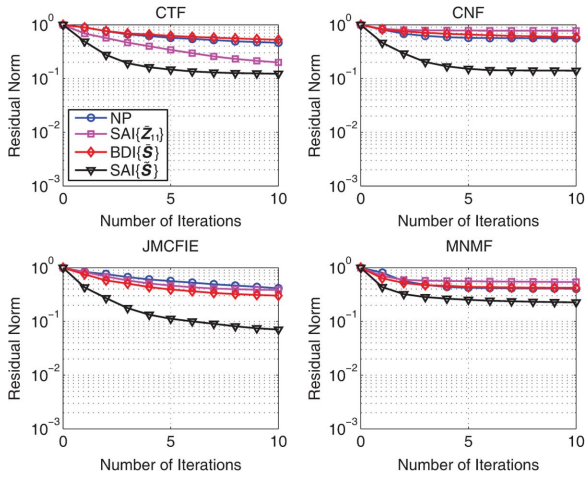

Fig. 5. Iterative solutions of (29) without preconditioning and with various preconditioners for the problem PW2 involving 162 420 unknowns.

results than CNF and MNMF, and it is also superior to these formulations in terms of efficiency with simple preconditioners [24]. Hence, JMCFIE can be considered as an alternative formulation to CTF.

For the solution of PhC problems, we use GMRES with ASP and FGMRES with ISP, without a restart in both the cases. Using GMRES-type solvers, the number of matrix–vector multiplications via MLFMA is the same as the number of iterations. For ISP1 and ISP2, there are also inner solutions involving matrix–vector multiplications with sparse near-field matrices. We note that these multiplications are much faster than the ordinary multiplications by MLFMA for the outer solutions. GMRES stores a sequence of orthogonal vectors to span the Krylov subspace; hence, its memory requirement increases linearly with the number of iterations. In order to provide the required flexibility, FGMRES has to store two sets of vectors, which increase the memory requirement. Nevertheless, the memory required for GMRES or FGMRES is usually negligible compared with the memory required for MLFMA and preconditioners. Except for PW3 and PW4, all solutions are performed sequentially on

TABLE III
SOLUTIONS OF PHC PROBLEMS INVOLVING PSS USING ALGEBRAIC PRECONDITIONERS

	NP		ILU(0)		ILUTP	
CTF	NoI	TST	NoI	TST	NoI	TST
PS1	473	1.6	186	0.6	409	2.2
PS2	†	†	335	2.7	702	8.4
PS3	†	†	353	5.1	†	†
PS4	†	†	*237	7.0	NA	
	4PBDP		ILU(0)		ILUTP	
JMCFIE	NoI	TST	NoI	TST	NoI	TST
PS1	149	0.5	87	0.3	124	1.2
PS2	107	0.9	175	1.4	205	4.3
PS3	276	4.0	197	2.9	244	17
PS4	698	21	408	12	‡	‡

NoI: Number of iterations. TST: Total solution time in hours. †: Iterations do not converge. ‡: Memory limit is exceeded. *: False convergence.

an Intel Xeon 5355 processor with 16 GB memory. PW3 and PW4 are solved on an Intel Xeon E5345 processor with 32 GB memory. In all problems, near-field and far-field interactions are calculated with maximum 1% error [24]. In iterative solutions, we set the initial guess as the zero vector, and stop the iterations when the residual error is reduced to less than 10^{-3} or when the number of iterations exceeds 1000. For the inner solutions of ISP, we set the residual error to 0.1 and the maximum number of inner iterations to 3 or 5, depending on the problem.

A. *Solutions of the PSs Problems*

First, we compare algebraic preconditioners, namely, the four-partition block-diagonal preconditioner (4PBDP) [24] and two ILU-type preconditioners for the solution of PhC problems involving PSs. 4PBDP is constructed from the diagonal blocks corresponding to the self-interactions of the lowest level clusters. This preconditioner is not used for CTF since it decelerates the convergence of this formulation. Instead, CTF is solved without preconditioning (NP). From the family of ILU-type preconditioners, we use ILU(0) and ILU with threshold and pivoting (ILUTP) [31], [32]. For ILUTP, we use a special set of parameters such that its memory requirement is approximately the same as that of ILU(0) [32]. We achieve this by using a low threshold value, i.e., 10^{-4}, and by setting the maximum number of nonzero elements per row to the average number of nonzero elements per row of the near-field matrix.

Table III presents the number of iterations and the total solution time (including the setup of the preconditioner and iterations) for the PSs problems listed in Table I. When the problems are formulated with CTF, convergence cannot be achieved in 1000 iterations without preconditioning for the larger three problems PS1, PS2, and PS3. For this formulation, ILU(0) significantly accelerates the iterative solutions, but this preconditioner leads to a false convergence for the largest problem PS4. In fact, for this problem, the *condest* value, which can be used to estimate the condition number of the incomplete factors, is 1.2×10^6, indicating the instability of the factorization. ILUTP

TABLE IV
SOLUTIONS OF PHC PROBLEMS INVOLVING PSS USING SCHUR-COMPLEMENT PRECONDITIONERS

$\tilde{\boldsymbol{S}}^{-1}$	SAI$\{\bar{\boldsymbol{Z}}_{11}\}$		SAI$\{\tilde{\boldsymbol{S}}\}$		SAI$\{\tilde{\boldsymbol{S}}\}$	
	ISP1(5)		ASP		ISP2(3)	
CTF	NoI	TST	NoI	TST	NoI	TST
PS1	107	0.5	104	0.6	109	0.6
PS2	210	2.2	216	2.2	206	2.3
PS3	358	6.3	490	7.7	386	6.7
PS4	933	33	†	†	964	34
	ISP1(5)		ASP		ISP2(5)	
JMCFIE	NoI	TST	NoI	TST	NoI	TST
PS1	53	0.3	106	0.6	54	0.4
PS2	47	0.7	207	2.1	45	0.9
PS3	112	2.2	233	4.0	116	2.5
PS4	388	14	558	18	344	13

NoI: Number of iterations. TST: Total solution time in hours. †: Iterations do not converge.

could produce more stable factors, but for both CTF and JMCFIE, this preconditioner does not accelerate the solutions compared to ILU(0). As expected, JMCFIE leads to faster solutions in comparison to CTF. Specifically, using the combination JMCFIE–ILU(0), the largest problem can be solved in 12 h.

In Table IV, we present the solution of PSs problems using Schur-complement preconditioners. In ISP1, we use $\mathrm{SAI}\{\bar{\boldsymbol{Z}}_{11}\}$ as a preconditioner for the solution of the reduced systems (28) and (29), and we set the maximum number of inner iterations to five. In ISP2, we employ $\mathrm{SAI}\{\tilde{\boldsymbol{S}}\}$ for the inner solution of the system (29), whereas (28) is still accelerated with $\mathrm{SAI}\{\bar{\boldsymbol{Z}}_{11}\}$. For the solution of CTF with ISP2, we set the maximum number of iterations to three since a further increase of this parameter does not reduce the iteration counts, but only leads to higher solution times. For JMCFIE, however, the optimal value is found be five, as in ISP1[1] . In addition to ISP1 and ISP2, we also employ ASP, based on the approximation of the inverse of $\bar{\boldsymbol{Z}}_{\mathrm{NF},11}$ with $\mathrm{SAI}\{\bar{\boldsymbol{Z}}_{11}\}$ and the inverse of $\bar{\boldsymbol{S}}$ with $\mathrm{SAI}\{\tilde{\boldsymbol{S}}\}$.

Comparing the results in Tables III and IV, we observe that PS4 formulated with CTF becomes solvable using ISP1 and ISP2 without any nonconvergence or false convergence problems. In addition, the smaller PSs problems PS1, PS2, and PS3 formulated with CTF are efficiently solved by using Schur-complement preconditioners. Particularly, PS1 and PS2 are solved more efficiently compared to solutions with algebraic preconditioners. For PS3, ILU(0) leads to the most efficient solutions, but Schur-complement preconditioners also perform well. The improvement of solutions is more visible in the case of JMCFIE. Specifically, ISP1 provides the fastest solutions of problems PS1, PS2, and PS3. For PS4 formulated with JMCFIE, ILU(0) leads to the most efficient solution, but the performance of ISP2 with a 13-h total solution time is close to the performance of ILU(0).

[1]Consequently, the total number of inner matrix–vector multiplications is equal to or less than five times the number of iterations for ISP1 and three or five times the number of iterations for ISP2.

TABLE V
MEMORY REQUIRED FOR THE SOLUTION OF PHC PROBLEMS INVOLVING PSS

	Preconditioner (MB)			MLFMA (MB)	
	ILU(0) & ILUT	ASP & ISP2	ISP1	CTF	JMCFIE
PS1	298	149	75	386	471
PS2	644	322	161	813	984
PS3	1038	519	260	1319	1608
PS4	2151	1075	538	2672	3249

TABLE VI
SOLUTIONS OF PHC PROBLEMS PW1 AND PW2 INVOLVING PW

$\tilde{\boldsymbol{S}}^{-1}$	-		-		SAI$\{\tilde{\boldsymbol{S}}\}$	
	NP		ILU(0)		ASP	
CTF	NoI	TST	NoI	TST	NoI	TST
PW1	695	0.7	141	0.3	58	0.3
PW2	†	†	†	†	217	3.6
	4PBDP		ILU(0)		ISP2(5)	
JMCFIE	NoI	TST	NoI	TST	NoI	TST
PW1	183	0.2	32	0.2	27	0.3
PW2	593	4.3	‡	‡	79	3.1

NoI: Number of iterations. TST: Total solution time in hours. †: Iterations do not converge. ‡: Memory limit is exceeded.

Finally, in Table V, we compare the memory required by the algebraic (ILU(0) and ILUT) and Schur-complement preconditioners for the solution of PhC problems involving PSs. Memory of 4PBDP is negligible and not included in the table. We observe that the memory required for the preconditioning is reduced by 50% using ISP2 and by 75% using ISP1, instead of ILU(0). We also note that these savings are significant considering the memory required for the MLFMA implementation itself, as also listed in Table V. Hence, in addition faster solutions, using ISP1 and ISP2 leads to more efficient solutions in terms of the memory usage compared to the ILU-type preconditioners.

B. Solutions of the PW Problems

In Table VI, we present the solution of the PW problems PW1 and PW2 listed in Table II. When the problems are formulated with CTF, solutions are accelerated with ILU(0) and ASP in addition to the NP case. For JMCFIE, we use 4PBDP, ILU(0), and ISP2, which are based on the acceleration of the inner solutions via $\mathrm{SAI}\{\tilde{\boldsymbol{S}}\}$. We observe that both ASP and ISP2 effectively improve the iterative solutions. For example, PW2 formulated with CTF cannot be solved (within 1000 iterations) even when using ILU(0). Using ASP, however, the solution can be obtained in less than 4 h. PW2 formulated with JMCFIE also cannot be solved with ILU(0) since the convergence is quite slow and the required memory exceeds the limit value before the residual error is reduced to below 0.001. The same problem can be solved in about 3 h using ISP2.

Solutions of PW3 and PW4 using Schur-complement preconditioners are listed in Table VII. These problems cannot be solved without preconditioning or with algebraic preconditioners, including ILU(0). In the case of ILU(0), convergence

TABLE VII
SOLUTIONS OF PHC PROBLEMS PW3 AND PW4 INVOLVING PWS

$\tilde{\boldsymbol{S}}^{-1}$	SAI$\{\tilde{\boldsymbol{S}}\}$			SAI$\{\tilde{\boldsymbol{S}}\}$	
	ASP			ISP2(5)	
CTF	NoI	TST	**JMCFIE**	NoI	TST
PW3	697	37	PW3	110	24
PW4	829	122	PW4	139	34

NoI: Number of iterations. TST: Total solution time in hours. †: Iterations do not converge. ‡: Memory limit is exceeded.

TABLE VIII
MEMORY REQUIRED FOR THE SOLUTION OF PHC PROBLEMS INVOLVING PWS

	Preconditioner (MB)		MLFMA (MB)	
	ILU(0)	ASP & ISP2	CTF	JMCFIE
PW1	643	321	764	852
PW2	4430	2215	4993	5509
PW3	15,905	7953	17,666	19,492
PW4	20,288	10,144	22,417	24,734

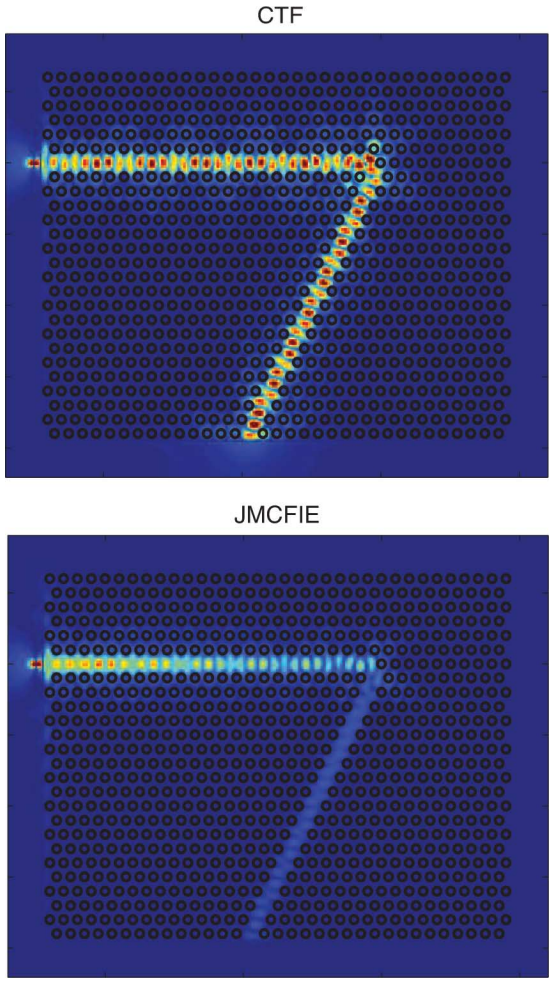

Fig. 6. Total magnetic field inside and in the vicinity of a 0.6 cm × 26 cm × 34 cm PW formulated with CTF and JMCFIE.

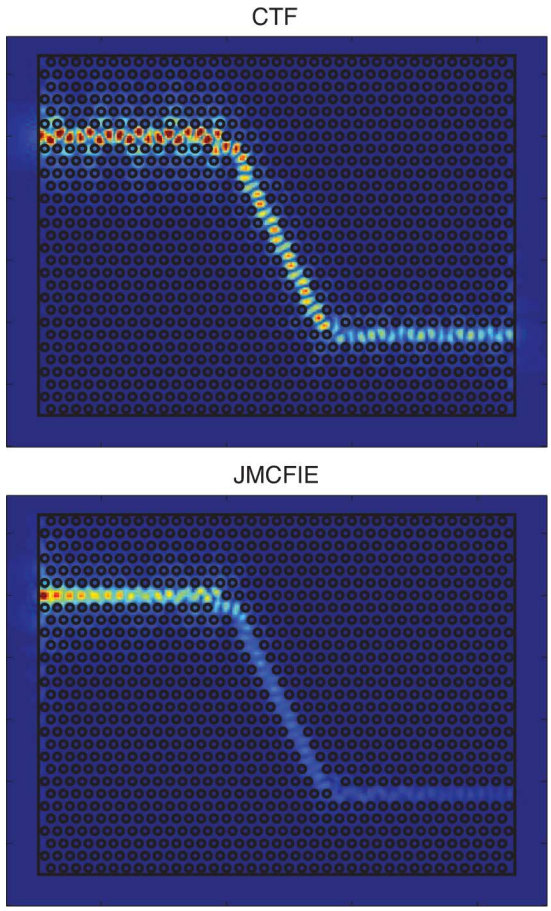

Fig. 7. Total magnetic field inside and in the vicinity of a 0.6 cm × 29 cm × 38 cm PW formulated with CTF and JMCFIE.

cannot be achieved before the limit memory of 32 GB is exceeded. On the other hand, using ASP for CTF and ISP2 for JMCFIE, both problems become solvable on the same computer. Specifically, the largest problem (PW4) involving 597 462 unknowns can be solved in 122 h using CTF–ASP and in 34 h using JMCFIE–ISP2.

Announcements of memory required for the solution of PhC problems involving PWs are listed in Table VIII. Similar to the PSs problems, using ASP or ISP2 reduces the preconditioner memory by 50% in comparison to ILU(0). This reduction is significant in the context of the total memory required for the MLFMA implementation.

Comparing the solutions for CTF and JMCFIE, one may conclude that JMCFIE is superior to CTF in terms of efficiency. Unfortunately, the accuracy of JMCFIE can be poorer compared to the accuracy of CTF. As an example, Figs. 6 and 7 present the normalized magnetic field inside and in the vicinity of the two larger PWs. We observe that JMCFIE solutions are significantly different than CTF solutions, especially toward the end of the waveguides. In fact, JMCFIE solutions could be misinterpreted as the inability of the waveguides to transmit the electromagnetic waves. However, as evident from the highly accurate results obtained with CTF, the waveguides operate perfectly and the electromagnetics waves are efficiently transmitted, as desired.

VI. Concluding Remarks

In this paper, we present rigorous solutions of PhC problems formulated with SIEs. Solutions are accelerated with MLFMA and novel Schur-complement preconditioners. From our numerical experiments, some of which are presented in this paper, we reach the following conclusions.

1) Considering the accuracy of solutions, CTF is superior to other formulations, including JMCFIE, especially for complicated PhC structures, such as a PW.
2) For relatively simple PhC problems, such as PSs, Schur-complement preconditioners are good alternatives to algebraic preconditioners. When the problem size is large, Schur-complement preconditioners are required, especially for CTF, which may not be solved with algebraic preconditioners.
3) For relatively complicated PhC problems, such as PWs, Schur-complement preconditioners are essential to accelerate solutions since algebraic preconditioners, including the ILU family, fail to provide efficient solutions.
4) Schur-complement preconditioners are shown to accelerate the solution of dielectric problems involving diverse permittivity values, both in this paper and more extensively elsewhere [33].
5) Considering both accuracy and efficiency of solutions, the combination of MLFMA, CTF, and Schur-complement preconditioners seems to be an ideal choice with which to investigate PhC problems.

To the best of authors' knowledge, dielectric PhC problems involving complicated, finite-sized (without infinite-periodicity homogenization approximation), 3-D geometries are analyzed for the first time with the reported levels of accuracy, efficiency, and detail. The fast SIE solvers and preconditioners reported herein are readily applicable to a wide variety of similarly complicated PhC problems.

References

[1] J. D. Joannopoulos, S. G. Johnson, J. N. Winn, and R. D. Meade, *Photonic Crystals, Molding the Flow of Light*. Princeton, NJ: Princeton Univ. Press, 2008.

[2] P. Loschialpo, D. W. Forester, and J. Schelleng, "Anomalous transmission through near unit index contrast dielectric photonic crystals," *J. Appl. Phys.*, vol. 86, no. 10, pp. 5342–5347, 1999.

[3] A. Mekis, J. C. Chen, I. Kurland, S. Fan, P. R. Villeneuve, and J. D. Joannopoulos, "High transmission through sharp bends in photonic crystal waveguides," *Phys. Rev. Lett.*, vol. 77, no. 18, pp. 3787–3790, Oct. 1996.

[4] S. G. Johnson, S. Fan, P. R. Villeneuve, and J. D. Joannopoulos, "Guided modes in photonic crystal slabs," *Phys. Rev. B*, vol. 60, no. 8, pp. 5751–5758, 1999.

[5] A. Talneau, P. Lalanne, M. Agio, and C. M. Soukoulis, "Low-reflection photonic-crystal taper for efficient coupling between guide sections of arbitrary widths," *Opt. Lett.*, vol. 27, no. 17, pp. 1522–1524, Sep. 2002.

[6] S. Boscolo and M. Midrio, "Three-dimensional multiple-scattering technique for the analysis of photonic-crystal slabs," *J. Lightw. Technol.*, vol. 22, no. 12, pp. 2778–2786, Dec. 2004.

[7] D. Pissoort, E. Michielssen, D. V. Ginste, and F. Olyslager, "Fast-multipole analysis of electromagnetic scattering by photonic crystal slabs," *J. Lightw. Technol.*, vol. 25, no. 9, pp. 2847–2863, Sep. 2007.

[8] R. Stoffer, H. J. W. M. Hoekstra, R. M. De Ridder, E. Van Groesen, and F. P. H. Van Beck Um, "Numerical studies of 2-D photonic crystals: Waveguides, coupling between waveguides and filters," *Opt. Quantum Electron.*, vol. 32, pp. 947–961, 2000.

[9] A. Mekis and J. D. Joannopoulos, "Tapered couplers for efficient interfacing between dielectric and photonic crystal waveguides," *J. Lightw. Technol.*, vol. 19, no. 6, pp. 861–865, Jun. 2001.

[10] M. Koshiba, "Wavelength division multiplexing and demultiplexing with photonic crystal waveguide couplers," *J. Lightw. Technol.*, vol. 19, no. 12, pp. 1970–1975, Dec. 2001.

[11] W. Kuang, W. J. Kim, and J. D. O'Brien, "Finite-difference time domain method for nonorthogonal unit-cell two-dimensional photonic crystals," *J. Lightw. Technol.*, vol. 25, no. 9, pp. 2612–2617, Sep. 2007.

[12] S. Venakides, M. A. Haider, and V. Papanicolaou, "Boundary integral calculations of two-dimensional electromagnetic scattering by photonic crystal Fabry–Perot structures," *J. Appl. Math.*, vol. 60, no. 5, pp. 1686–1706, May 2000.

[13] T.-L. Wu, J.-S. Chiang, and C.-H. Chao, "A novel approach for calculating the dispersions of photonic crystal fibers," *IEEE Photon. Technol. Lett.*, vol. 16, no. 6, pp. 1492–1494, Jun. 2004.

[14] J. Yuan, Y. Y. Lu, and X. Antoine, "Modeling photonic crystals by boundary integral equations and Dirichlet-to-Neumann maps," *J. Comput. Phys.*, vol. 227, no. 9, pp. 4617–4629, Apr. 2008.

[15] A. J. Poggio and E. K. Miller, , R. Mittra, Ed., "Integral equation solutions of three-dimensional scattering problems," in *Computer Techniques for Electromagnetics*. Oxford, U.K.: Pergamon, 1973, ch. 4.

[16] T. K. Wu and L. L. Tsai, "Scattering from arbitrarily-shaped lossy dielectric bodies of revolution," *Radio Sci.*, vol. 12, no. 5, pp. 709–718, Sep./Oct. 1977.

[17] Y. Chang and R. F. Harrington, "A surface formulation for characteristic modes of material bodies," *IEEE Trans. Antennas Propagat.*, vol. AP-25, no. 6, pp. 789–795, Nov. 1977.

[18] C. Müller, *Foundations of the Mathematical Theory of Electromagnetic Waves*. New York: Springer-Verlag, 1969.

[19] J. Song, C.-C. Lu, and W. C. Chew, "Multilevel fast multipole algorithm for electromagnetic scattering by large complex objects," *IEEE Trans. Antennas Propagat.*, vol. 45, no. 10, pp. 1488–1493, Oct. 1997.

[20] P. Ylä-Oijala, M. Taskinen, and S. Järvenpää, "Surface integral equation formulations for solving electromagnetic scattering problems with iterative methods," *Radio Sci.*, vol. 40, no. 6, RS6002, Nov. 2005, doi:10.1029/2004RS003169.

[21] P. Ylä-Oijala and M. Taskinen, "Well-conditioned Müller formulation for electromagnetic scattering by dielectric objects," *IEEE Trans. Antennas Propag.*, vol. 53, no. 10, pp. 3316–3323, Oct. 2005.

[22] P. Ylä-Oijala and M. Taskinen, "Application of combined field integral equation for electromagnetic scattering by dielectric and composite objects," *IEEE Trans. Antennas Propag.*, vol. 53, no. 3, pp. 1168–1173, Mar. 2005.

[23] S. M. Rao, D. R. Wilton, and A. W. Glisson, "Electromagnetic scattering by surfaces of arbitrary shape," *IEEE Trans. Antennas Propag.*, vol. AP-30, no. 3, pp. 409–418, May 1982.

[24] Ö. Ergül and L. Gürel, "Comparison of integral-equation formulations for the fast and accurate solution of scattering problems involving dielectric objects with the multilevel fast multipole algorithm," *IEEE Trans. Antennas Prop.*, vol. 57, no. 1, pp. 176–187, Jan. 2009.

[25] Ö. Ergül and L. Gürel, "Discretization error due to the identity operator in surface integral equations," *Comput. Phys. Comm.*, vol. 180, no. 10, pp. 1746–1752, Oct. 2009.

[26] M. Benzi, G. H. Golub, and J. Liesen, "Numerical solution of saddle point problems," *Acta Numer.*, vol. 14, pp. 1–137, 2005.

[27] Ö. Ergül and L. Gürel, "Efficient solution of the electric and magnetic current combined-field integral equation with the multilevel fast multipole algorithm and block-diagonal preconditioning," *Radio Sci.*, vol. 44, pp. RS6001-1–RS6001-15, Nov. 2009, RS6001, doi:10.1029/2009RS004143.

[28] E. Chow and Y. Saad, "Approximate inverse techniques for block-partitioned matrices," *J. Sci. Comput.*, vol. 18, no. 6, pp. 1657–1675, Nov. 1997.

[29] P. Ylä-Oijala, M. Taskinen, and S. Järvenpää, "Analysis of surface integral equations in electromagnetic scattering and radiation problems," *Eng. Anal. Boundary Elem.*, vol. 32, no. 3, pp. 196–209, Mar. 2008.

[30] C. Siefert and E. de Sturler, "Preconditioners for generalized saddle-point problems," *J. Numer. Anal.*, vol. 44, no. 3, pp. 1275–1296, 2006.

[31] Y. Saad, *Iterative Methods for Sparse Linear Systems*. Philadelphia, PA: SIAM, 2003.

[32] T. Malas and L. Gürel, "Incomplete LU preconditioning with multilevel fast multipole algorithm for electromagnetic scattering," *J. Sci. Comput.*, vol. 29, no. 4, pp. 1476–1494, Jun. 2007.

[33] T. Malas and L. Gürel, "Schur complement preconditioners for surface integral-equation formulations of dielectric problems solved with the multilevel fast multipole algorithm," *SIAM J. Sci. Comput.*, 2011, to be published.

Özgür Ergül (S'97–M'09) received B.Sc., M.S., and Ph.D. degrees from Bilkent University, Ankara, Turkey, in 2001, 2003, and 2009, respectively, all in electrical and electronics engineering.

He is currently a Lecturer in the Department of Mathematics and Statistics, University of Strathclyde, Glasgow, U.K. He is also a Lecturer at the Centre for Numerical Algorithms and Intelligent Software, which is an Engineering and Physical Sciences Research Council/Scottish Funding Council (SFC) funded Centre. From 2001 to 2009, he was a Teaching and Research Assistant in the Department of Electrical and Electronics Engineering, Bilkent University, where he was with the Computational Electromagnetics Group from 2000 to 2005, and with the Computational Electromagnetics Research Center from 2005 to 2009. His research interests include fast and accurate algorithms for the solution of electromagnetics problems involving large and complicated structures, integral equations, parallel programming, iterative methods, and high-performance computing.

Dr. Ergul is a recipient of the 2007 IEEE Antennas and Propagation Society Graduate Fellowship, the 2007 Leopold B. Felsen Award for Excellence in Electrodynamics, and the 2010 Serhat Ozyar Young Scientist of the Year Award.

Tahir Malas (M'06) received the B.Sc. degree in electrical and electronics engineering from the Middle East Technical University, Ankara, Turkey, in 2000, the M.Sc. degree from the Department of Computer Engineering, Bilkent University, Ankara, in 2004, and the Ph.D. degree from the Department of Electrical and Electronics Engineering, Computational Electromagnetics Research Center, Bilkent University, in 2010.

He is currently a Postdoctoral Fellow at The University of Texas at Austin, Austin. He was engaged in industry for one year. He is the author or coauthor of more than 40 published journal and conference papers in areas concerning his research interests. His research interests include biolectromagnetics, preconditioning methods for integral-equation methods, and parallel computing.

Levent Gürel (S'87–M'92–SM'97–F'09) received the B.Sc. degree from the Middle East Technical University, Ankara, Turkey, in 1986, and the M.S. and Ph.D. degrees from the University of Illinois at Urbana-Champaign (UIUC),Urbana, in 1988 and 1991, respectively, all in electrical engineering.

In 1991, he was a Research Staff Member at Thomas J. Watson Research Center, International Business Machines Corporation, Yorktown Heights, NY, where he was engaged in research on electromagnetic compatibility (EMC) problems related to electronic packaging, use of microwave processes in the manufacturing and testing of electronic circuits, and the development of fast solvers for interconnect modeling. Since 1994, he has been a faculty member in the Department of Electrical and Electronics Engineering, Bilkent University, Ankara, where he is currently a Professor. In 1997, he was a Visiting Associate Professor at the Center for Computational Electromagnetics, UIUC, for one semester, where he was a Visiting Professor in 2003–2005, and an Adjunct Professor after 2005. He founded the Computational Electromagnetics Research Center, Bilkent University, in 2005, where he is the Director. Since 2006, his research group has been breaking several world records by solving extremely large integral-equation problems, involving hundreds of millions of unknowns. His research interests include the development of fast algorithms for computational electromagnetics and the application thereof to scattering and radiation problems involving large and complicated scatterers, antennas and radars, frequency-selective surfaces, high-speed electronic circuits, optical and imaging systems, nanostructures, metamaterials, electromagnetic compatibility and interference, subsurface scattering, and ground penetrating radars.

Dr. Gürel is the recipient of the Turkish Academy of Sciences (TUBA) Award in 2002, and the Scientific and Technical Research Council of Turkey (TUBITAK) Award in 2003. He is a member of the United States National Committee of the International Union of Radio Science (URSI), and the Chairman of Commission E (Electromagnetic Noise and Interference) of URSI Turkey National Committee. He was a member of the General Assembly of the European Microwave Association during 2006–2008. He is currently an Associate Editor for *Radio Science*, IEEE ANTENNAS AND WIRELESS PROPAGATION LETTERS, *Journal of Electromagnetic Waves and Applications*, and *Progress in Electromagnetics Research*. He was also the Chairman of the AP/MTT/ED/EMC Chapter of the IEEE Turkey Section in 2000–2003. In 2000, he founded the IEEE EMC Chapter in Turkey. He was the Cochairman of the 2003 IEEE International Symposium on Electromagnetic Compatibility. He is the organizer and General Chair of the CEM International Workshops held in 2007 and 2009. During 2011–2013, Dr. Gürel is serving as an IEEE Distinguished Lecturer and on the Board of Directors of Applied Computational Electromagnetics Society (ACES).